Journal of Solid Mechanics Vol. 7, No. 3 (2015) pp. 268-280

Investigation on the Effect of Tigthening Torque on the Stress Distribution in Double Lap Simple Bolted and Hybrid (Bolted -Bonded) Joints

F. Esmaeili [1, *] , T.N. Chakherlou [2]

[1]*Department of Mechanical Engineering, Tabriz Branch, Islamic Azad University, Tabriz, Iran*
[2]*Faculty of Mechanical Engineering, University of Tabriz, P.O. Box 51666-14766, Tabriz, Iran*

Received 29 May 2015; accepted 5 July 2015

ABSTRACT

In this research, the effects of torque tightening on the stress distribution in double lap simple bolted and hybrid (bolted-bonded) joints have been investigated numerically. In order to determine the bolt clamping force value due to tightening torque in simple bolted and hybrid joints, which is necessary in numerical simulation, an experimental approach has been proposed. To do so, two kinds of joints, i.e. double lap simple and hybrid joints were prepared. To determine the bolt clamping force or pretension resulting from the torque tightening, at different applied torques, for both kinds of joints a special experimental method was designed using a steel hollow cylinder that was placed between the nut and the plate. In order to obtain the stress distribution in the joint plates for both kinds of the joints, with two different amounts of tightening torque, three-dimensional finite element models were simulated by a general finite element code. The obtained results revealed that the amounts of resultant stresses were reduced by increasing the tightening torque due to compressive stresses. Furthermore, in the hybrid joints, the stress concentration around the hole is reduced significantly. Finally, the comparison of the obtained results, confirms that the hybrid joints have better static strength than simple joints for all levels of the tightening torque.

Keywords : Clamping force; Bolted joint; Hybrid joint; Tightening torque; Hook's law.

1 INTRODUCTION

MOST of machines and structures have various types of joints (such as mechanical fastening, welding and bonded joints) for the effective productivity and maintainability. Detachable joints such as bolts, rivets or pins are frequently used to create assemblies or structures from detailed parts or structural elements. Among the mentioned detachable joints, bolted joints are widely used in mechanical structures. A key advantage of threaded fasteners over the majority of other joining methods is that they can easily be disassembled and re-used. This feature is often the reason why threaded fasteners are used in preference to other joining methods. Nevertheless, mechanically fastened connections do have several attributes that are cause for concern. For example, because of the existence of geometrical discontinuity as a consequence of essential hole drilling operation in bolted joints results in stress concentration and thus increases the tendency of fatigue crack to initiate and grow under cyclic loading [1-3].

* Corresponding author. Tel.: +98 411 3392492; Fax: +98 411 3354153.
E-mail address: f.esmaeili@iaut.ac.ir (F. Esmaeili).

In order to overcome this problem, the structure frequently needs to be thickened locally. This added thickness, together with the high volume of metallic fasteners, increases the weight of structure, and so decreases the strength to weight efficiency ratio.

A substitute method to mechanical fastening is adhesive bonded joints. Adhesively bonded joints of aluminum alloys in lap joints should be useful in comparison with mechanical bolted joints. In order to see the benefits of adhesively bonded joints under the fatigue loading, two important differences among the mechanical and bonded joints are significant. Primarily, in a mechanical joint, the overlapping areas are attached to one another at discreet points only, i.e. by the fasteners. Clearly, severe stress concentrations should occur. However, if the connection is made continuously in the full overlapping area by adhesive bonding, these stress concentrations do not occur. Because, the fastener and required holes are avoidable in the bonded joints. Therefore, the stress distributions in the joint are relatively uniform in comparison with those in the mechanical joint. Secondly, metallic contact between the two sheets is absent in the adhesively bonded joints, and thus fretting between the mating sheets is also eliminated [4].

Adhesively bonded joints are extensively used for different engineering applications, such as aerospace structures, automotive and marine industries and etc. Tensile loads on the bonded joints usually eluded due to the occurrence of peeling failures. Nevertheless, the static and fatigue strength at shear loading are acceptable [4].

Like mechanical fastening joints, adhesively bonded connections also have their own disadvantages associated with the method and performance.

The adhesively bonded connections, in comparison to mechanically fastened joints, are more difficult to manufacture in instances where the adhesive layer thickness is critical. Furthermore, the adhesive joints are more difficult to inspect than mechanical joints, as visual inspection is often not an effective way to detect damage, as damage within the adhesive is not visible from the surface.

In order to reduce the weakness and disadvantages of adhesive bonding, and mechanical joints, and therefore, to obtain high performance joints, a combination of a mechanical joints (riveted, bolted etc.) with an adhesive, namely hybrid joints, are used [4-7]. Hybrid joints are used in many engineering application such as aerospace, automotive, and naval industries due to better performance of hybrid joints compared to simple joints [8]. Hybrid joints have also been used for the repair and improvement of damage tolerance [9]. The hybrid joints may include weld-bonded, clinch-bonded and rivet-bonded connections. It is important to emphasize that, although some limited research have been done on the analysis of hybrid joints, still static and fatigue strength data for the hybrid joint are lacking.

The hybrid joint method has been studied by several researchers [10-15]. An analytical investigation was conducted by Hart-Smith [7] on a hybrid joint with stepped lap joints between titanium and carbon fiber reinforced plastic adherends. The strength of hybrid joints was found to be the same as well-designed bonded joints. In the peripheral of this problem, many researchers proposed different numerical methods and analytical solutions to analyze hybrid joints. Chan and Vedhgiri [10] conducted experiments with composite joints as well as a parametric study using finite element analysis to study the stacking sequence effect on joint strength. In that work, it was also found that bolts do not take an active role in load transfer before the initiation of failure in bonding, which was also noted by Hart-Smith [7]. Barut and Madenci [12] developed a semi-analytical solution method for stress analysis of a hybrid joint, and found that most of the load is transferred through the adhesive, even though it has low modulus as compared to the bolt. Kweon et al. [15] observed a similar phenomenon in their experiments, where a double lap hybrid joint was considered using composite and aluminium adherends.

One of the most important factors that influence the strength of a bolted joint is the amount of pre-tension or clamping force resulting from the tightening torque that applied to the bolt. Preload or clamping force in the bolt is achieved by using a torque wrench. The torque wrench applied torque to the nut or the head of the bolt. This applied torque correlates with induced tension or clamping force [16-20].

Computations indicate that the torque required to induce clamping force F_{cl} in the bolt, for standard threads, can be presented approximately by the following equation:

$$T=KF_{cl}d \tag{1}$$

where T, F_{cl} and d are the applied tightening torque to the bolt head or nut, the clamping force and the nominal thread diameter, respectively, and K represents the torque coefficient or nut factor which depends on a variety of parameters including but not limited to geometry and friction of the threads [20].

Previous works revealed that the clamping force can reduce the stress concentration at the bolted hole region, and therefore improve the strength of the joint considerably [16,17,19, 21]. In an experimental investigation, Sekercioglu and Kovan [18] have studied the effects of different coated bolts, three different bolt diameters, and coarse and fine pitch on torque strength of bolted connections with locked anaerobic adhesive. Collings [23] has

discussed the effects of variables such as laminate thickness and bolt clamping pressure on the strength of bolted joints in CFRP laminates. Stockdale and Matthews [24] investigated the effect of clamping pressure on bolt bearing load in glass fiber-reinforced plastics experimentally. Deng and Hutchinson [25] investigated the residual clamping stress exerted by the rivets on the joint. Relation between the clamping and applied force was analyzed using finite element methods in the small strain framework. Nah et al. [26] suggested an approach for estimating the clamping force of bolts subjected to temperature gradient.

In this study, the effects of torque tightening on the stress distribution in simple and hybrid joints have been investigated numerically. In order to obtain the stress distribution in the joint plates for both kinds of the joints, with two different amounts of tightening torque, three-dimensional finite element models were simulated by a general finite element code.

In addition, the relationships between the applied torques and the clamping forces in double lap simple bolted and hybrid (bolted-bonded) joints will be investigated experimentally. To do so, two kinds of joints, i.e. double lap simple and hybrid (bolted-bonded) joints were considered to carry out experiments. To determine the bolt clamping force or pretension resulting from the torque tightening, at different applied torques, for both kinds of joints a bolt transducer made of steel was designed using a hollow cylinder with two strain gages which attached on the outer surface of the hollow cylinder. This transducer was located between the connection plate and nut. The suitable strain gauge boxes were used to read the strains values of attached strain gauges as a result of the induced axial strain from the torque tightening and therefore pretension or clamping force of bolts was calculated by means of Hooke's elasticity law.

2 EXPERIMENTAL PROCEDURES

The specimens employed in this investigation were constructed using 2 mm thick 2024-T3 aluminium alloy. The aluminum alloy 2024-T3, is widely used in the structures of aircrafts. Table 1. lists the mechanical properties of the aluminium alloy obtained from tension (static) tests, and the chemical compositions of used aluminium alloy are illustrated in Table 2.

Table 1
Mechanical properties of aluminium 2024-T3 alloy**.**

Young Modulus GPa	Yield Strength MPa	Tensile Strength MPa	Poisson's Ratio	Elongation %
72	315	550	0.33	18

Table 2
Chemical composition of aluminium 2024-T3 alloy (% weight)**.**

Cu	Mg	Mn	Si	Cr	Zn	Ti	Al
4.82	1.67	0.58	0.07	0.02	0.06	0.15	Balance

Two different kinds of joints i.e. double lap simple and hybrid (bolted-bonded) joints were prepared. Test specimens' configurations and dimensions for both kinds of joints have been illustrated schematically in Fig.1.

The hybrid joints were fabricated using the structural two component epoxy adhesive, namely Loctite 3421[27], prepared by mechanical mixing of the resin and hardener in equal amount by weight. The adhesive was selected due to its high strength and long working life. Before preparation of all of the specimens, to eliminate any possible surface scratches, the surfaces of the plates, were polished mechanically by rubbing with different grinding papers, identified by grit 400 then 600 and finally 1000.

In order to obtain the tensile stress-strain curve of the adhesive, several dog-bone specimens were prepared according to ASTM D638-02. The adhesives were injected into a mold , as shown in Fig. 2, and left to cure at room temperature for 24 hours. Finally, the prepared specimens were tested on a 100 kN Zwick/Z100 static testing machine with a crosshead speed of 5 mm/min (see Fig. 3). The engineering stress–strain curve of the adhesive is shown in Fig. 4.

To prepare the simple specimens, fastener holes of diameter of 5 mm, were drilled and reamed in the jointed plates. Bolt used in this experiment had hexagonal head and a typical 5 mm shank diameter, which was then paired with hexagonal nut. Circular washer was used under both the hexagonal head and nut. The optimum length of the un-threaded part of the shank was selected in order to match the thickness of the plates to be joined, so that the

contact between the plates and the bolts is along the un-threaded part of the shank. Finally, the nut is tightened by applying torque using a torque-wrench up to required amounts of torques.

As mentioned earlier, aluminium alloy 2024-T3 sheets were used as an adherend for preparation hybrid joints in this investigation. The preparation of the hybrid joints has been implemented in two main steps. Firstly, a double lap bonded joint was constructed. In order to obtain high strength joint, the jointed plates were cleaned with acetone and then were allowed to dry, prior to the application of the adhesive layer. In order to achieve the constant thickness of adhesive layer, 0.5 mm thickness sheets were used between adherends.

The prepared bonded joints were left in ambient temperature for 72 hours, in accordance with the adhesive manufacturer. To delete the effects of fillets ,thereafter, the fillets of bonded joints were removed with a razor.

The second step of preparing the hybrid joints was done using the same procedures of preparation of the simple bolted joints. In this step, the bolts were tightened using the same amounts of torques as the simple bolted joints.

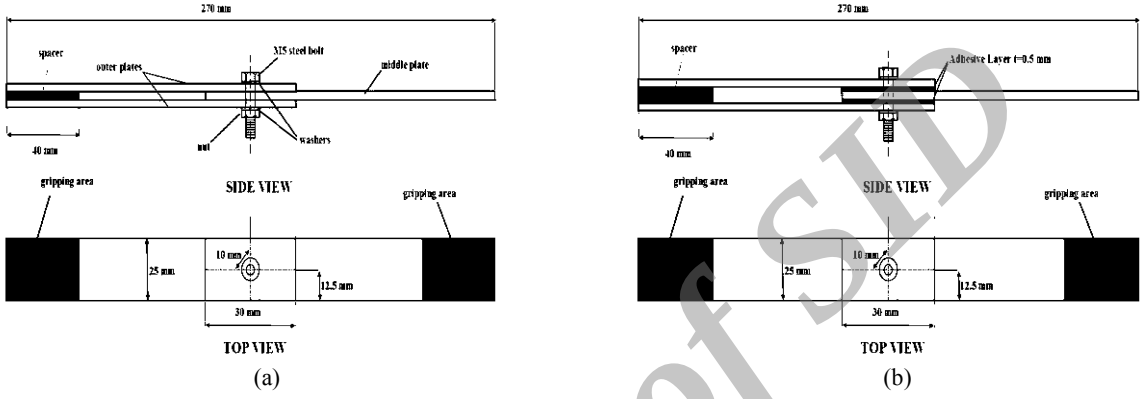

Fig.1
Configurations and dimensions of the joints. (a) Simple bolted joint, (b) Hybrid (bonded- bolted) joint.

Fig.2
Mold for dog-bone specimens.

Fig.3
The adhesive dog-bone specimen under tensile testing.

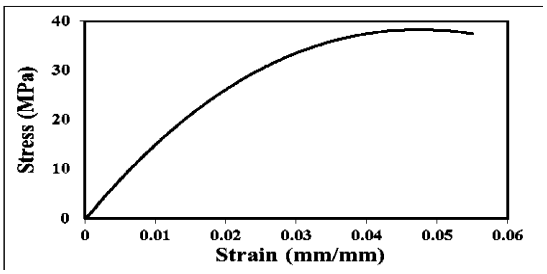

Fig.4
Engineering stress-strain curve of Loctite 3421 adhesive.

2.1 Clamping force measurement

To insure that the used bolts and nuts are in the elastic region, a number of preliminary tests were conducted and the obtained results indicated that initial plastic strain started at approximately 8 Nm at threads [28]. In order to measure the clamping force or pretension resulting from the torque tightening, under different applied torques, for both kinds of joints, i.e. simple bolted and hybrid joints, a bolt transducer which located between the plate and nut was used. Fig.5 illustrates the dimensions of used transducer. This bolt transducer consists of a hollow cylinder with two strain gages attached on its outer surface (as shown in Fig.6). The suitable strain gauge boxes were used to read the strains values of attached strain gauges as a result of the induced axial strain from the torque tightening and therefore pretension or clamping force of bolts was calculated by means of Hooke's elasticity law. The proposed approach for assessing the pretension in the bolt and the hollow cylinder dimensions were illustrated in Fig.7.

In order to obtain relationship between the applied torque and clamping force, torques were applied in 1 Nm increments from 1 to 7 Nm to the nut using a torque wrench, and then the axial strains were recorded for each value of the torques. This test was repeated three times for each case to obtain the average amount of compressive strains (ε_m), and determine the corresponding clamping forces using Eq. (2) as follows:

$$F_{cl} = E_C A_C \varepsilon_m = 204188 \times \frac{\pi}{4}(9^2 - 5^2)\varepsilon_m = 89.8 \times 10^5 \varepsilon_m (N) \tag{2}$$

In the above equation, A_C is the area of the hollow cylinder cross section. The elastic modulus for the hollow cylinder material (E_C) was also experimentally determined in order to obtain the accurate values for the mean axial clamping force.

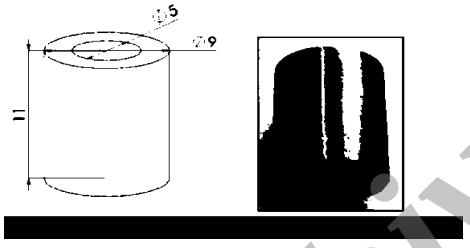

Fig.5
Dimensions of used transducer.

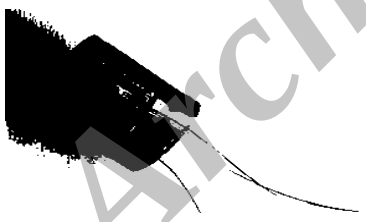

Fig.6
Strain gages attached on used transducer.

Fig.7
Measuring clamping force with load cell.

3 NUMERICAL ANALYSIS

In order to obtain the stress distribution in the joint plates for both kinds of the joints, with two different amounts of tightening torque (1, and 5 Nm), three-dimensional finite element models were simulated by ANSYS 9.0 general finite element code [29]. All of the adherends and adhesive layer are meshed with eight-node hexahedral structural solid elements Solid45. The finite element mesh of the double lap hybrid joint specimens is presented in Fig. 8, together with its corresponding loading and boundary conditions. The nodes located at the left edge of the FE model were considered to have all their degrees of freedom constrained. Only one quarter of the specimen has been modelled, due to double symmetry (with respect to *X-Z* and *X-Y* Cartesian planes) and symmetric displacement boundary condition has been applied to the corresponding planes as shown in the figure. The bottom face of the bolt shank was used to implement the bolt clamping force.

In order to transfer the pressure between the contacting surfaces, flexible-to-flexible contact state was used. The friction effect between the surfaces of the washer (bolt head) and Al-alloy plate was included in the FE model using Elastic Coulomb model with friction coefficient of μ=0.29 which was obtained from experimental tests based on sliding of the washer under its own weight on the sloped surface from Al-alloy plate. Also based on the similar experiments, the friction coefficient was found to be μ=0.4 for the contact between the plates.

It must be noted that, in an investigation has been carried out by De Angelis [30] a comparative analysis has been presented among the linear and the nonlinear kinematic hardening assumptions for defining material behaviour in elasto-plastic region using illustrative numerical simulations. Numerical analyses and results have been reported which allow comparing for different simulations the suitability of the assumptions of linear versus nonlinear kinematic hardening rules for elasto-plastic materials. Truthfully, in finite element applications of large scale elasto-plastic structural analysis the linear kinematic hardening rule is usually accepted. Because, this assumption leads to a symmetric tangent stiffness matrix and time consuming solution procedures. Nevertheless, in the literature it has been discussed the opportunity of assuming nonlinear kinematic hardening rules in order to properly simulate experiments on real materials. The computational implementation and research for fast and effective numerical procedures for nonlinear kinematic hardening rules is not insignificant particularly for large structural simulations and complex loading conditions which involve large computing times [30-32]. Therefore, in current study, in order to characterize the aluminium alloy 2024-T3 stress–strain behaviour, an elastic–plastic multi-linear kinematic hardening material model with Von Mises criterion was used. This behaviour of the material was obtained from simple tensile tests and shown in Fig. 9. The elastic modulus and Poisson's ratio were measured to be E = 72 GPa and ν = 0.33 respectively. Also, for adhesive layer the multi-linear isotropic material model was used and the Poisson's ratio was considered equal to 0.35. Moreover, for the steel bolt a linear elastic material relation was assumed with Young's modulus of 207 GPa and Poisson's ratio of 0.30 as it was observed that the bolt material remained in elastic region when it was subjected to maximum applied torque (8 Nm).

Finite element analyses were implemented in two main steps including the application of the clamping force which was followed by a longitudinal load to the end of main plate. In the first step of loading, axial displacement was applied to the bottom face of the bolt shank to simulate the clamping force. This process was completed for two initial clamping forces resulting from the different amounts of tightening torques for both kinds of the joints using a trial and error method. In the second step, the value of longitudinal tensile load was applied to the end of the main plate in the model.

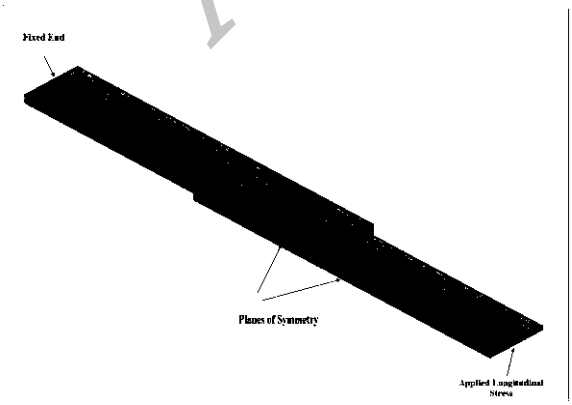

Fig.8
Applied loads and boundary conditions in three dimensional finite element model.

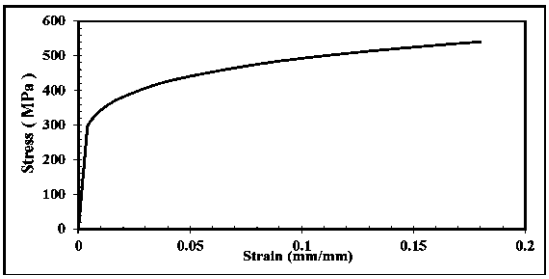

Fig.9
True stress-strain curve of 2024-T3 aluminium alloy.

4 RESULTS AND DISCUSSIONS

4.1 The relationship among the applied tightening torque and the clamping force

As mentioned in previous section, in order to measure the clamping force resulting from tightening torque, two different kinds of specimens, i.e. double lap simple and hybrid (bolted-bonded) joints were prepared. To do so, a bolt transducer which located between the plate and nut was used. This bolt transducer consists of a hollow cylinder with two strain gages attached on its outer surface. The suitable strain gauge boxes were used to read the strains values of the attached strain gauges as a result of the induced axial strain from the torque tightening and therefore pretension or clamping force of bolts was calculated by means of Hooke's elasticity law. Finally, the axial force in the hollow cylinder and then the clamping force have been determined. The relationship between the applied tightening torque and the average amount of compressive strains for both kinds of joints, are given in Fig. 10.

The relationship among the calculated clamping forces using Eq. (2) and the applied tightening torques for both kinds of joints are shown in Fig. 11. As it can be seen from this figure, there is a linear relationship among the calculated clamping force and the applied tightening torque. This indicates that the hollow cylinder material deforms elastically, for all levels of applied tightening torques.

According to the achieved linear relationship on the graph and Eq. (1), the torque coefficient K can be calculated for the double lap simple bolted joint as follows:

$$\frac{1}{k(5\times10^{-3})} = 987.8 \;\rightarrow\; k = 0.202 \tag{3}$$

In order to obtain relationship among the applied tightening torques and clamping force in the case of double lab hybrid joints, same experiments were similarly conducted for the hybrid specimen. For the purpose of making comparison between the clamping forces resulting from the same tightening torques in the two different kinds of joints, the obtained results have been displayed in Figs. 10 and 11.

The torque coefficient K can be calculated for the double lap hybrid bolted joint using the linear equation on the graph and Eq. (1), as follows:

$$\frac{1}{k(5\times10^{-3})} = 841.43 \;\rightarrow\; k = 0.238 \tag{4}$$

For the case of the double lap hybrid joint, the torque coefficient K is obtained equals to 0.238, according to Eq. (1), and the obtained linear equation on the graph.

As it can be seen from the Fig. 11, the torque required to obtain a specific value of clamping force, was significantly lower in double lap simple bolted joints in comparison with the hybrid joints. In other words, the clamping force corresponds to a specific value of tightening torque in hybrid joints is lower than the obtained clamping force at the same value of tightening torque in simple bolted joints. Also, based upon the torque and clamping force relationship and the dimensions of the bolt, and according to the Eq. (1), the torque coefficient K was determined for the double lap hybrid bolted joint. It can be found that the torque coefficient increases from 0.202 to 0.238, for the simple bolted and hybrid joints, respectively.

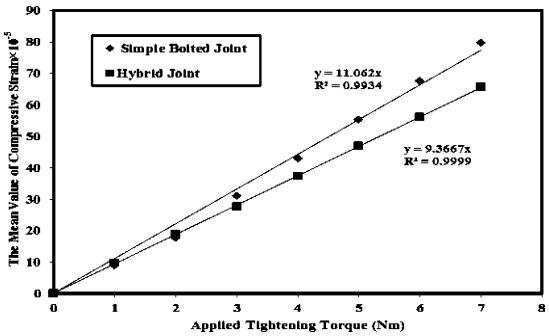

Fig.10
The relation between the applied tightening torque and the mean value of compressive strains.

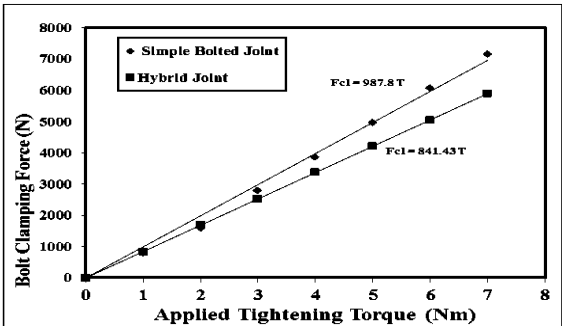

Fig.11
The Tightening torque-clamping force relation.

4.2 Stress distribution in the main plate

As it was mentioned previously, two different tightening torque values were selected to be applied. To do so, the corresponding clamping force, i.e. $F_{cl} = 976$, and 4880 N for simple bolted joints, and F_{cl}=840, and 4200 N for hybrid joints were to be applied on the plates. Therefore, a displacement boundary condition in –Z direction was applied on the lower face of the bolt shank to achieve the desired clamping forces equal to experimental test results. The magnitude of the required displacement was found after a few trial and error processes to achieve the desired clamping forces resulting from tightening torques.

According to the results of the first load step solution of the finite element analysis, some compressive stresses were observed near the hole of the joints. The compressive stress contours around the bolt hole of the main plate, created due to 1, and 5 Nm tightening torques are shown in Fig. 12. As it can be seen, the most compressive stresses are observed at the edge of the hole which increased from -20 to -101 MPa when the tightening torque increased from 1 to 5 Nm in simple bolted specimens. In addition, in case of the hybrid joints, the amount of compressive stress increased from -13 to -49 MPa when the tightening torque increased from 1 to 5 Nm.

In the second load step, a tensile remote stress was applied to the FE models to simulate the tensile loading of the specimens. Therefore, a tensile (remote) stress equal to 192 MPa was applied on the right end of the main plate while the displacement of the left end of the connector plates was constrained.

The contour of longitudinal normal stress σ_x due to different tightening torque and applied remote longitudinal tensile stress of 192 MPa are shown in Fig. 13 for both kinds of the joints.

As expected, the maximum stress values occurred at the edge of the hole which decreased from 428 to 398 MPa for simple bolted specimens and 324 to 261 MPa for hybrid specimens when the tightening torque increased from 1 to 5 Nm.

In order to compare the considered kinds of joints and investigate the effect of bolt tightening torque, the stress distributions have been plotted. The stress distributions through the two different paths (as shown in Fig. 14) in the top and mid planes of main plate, for both kinds of the joints, have been plotted. The resultant longitudinal stress distribution, σ_x , and distribution of Normal stress, σ_z, in these paths are shown in Figs. 15 and 16 for different tightening torques under the application of maximum remote stress equals to $S_{\max} = 192$ MPa, respectively.

As be shown in Fig. 15, increasing the applied tightening torques, considerably, decreases the values of longitudinal stress, σ_x, in case of simple bolted joints. However, in the case of hybrid joints, this effect is less in

comparison with simple bolted joints. Additionally, it can be observed from these figures that the maximum amount of longitudinal stress, σ_1, in hybrid bolted joints, was several times lower in comparison to the simple bolted joints. Furthermore, it can be seen from these figure, that the hybrid joints create a uniform stress distribution on overlap length.

A similar behavior can be observed from distribution of normal stress, σ_z, in Fig. 16. As it can be seen from Fig. 16, increasing the tightening torque, leads to a significant increase in the values of normal stress, σ_z, as expected. According to the Fig. 14, the compressive stress due to clamping force as a result of tightening torque, concentrated the normal stress distribution near the hole of the joint in the case of simple bolted joints. However, in the case of the hybrid joints the compressive stress is distributed uniformly on the overlap area due to presence of adhesive layer.

Finally, the first principal stress distribution, σ_1, in the paths 1, and 2 are shown in Figs. 17 for different tightening torques under the application of maximum remote stress.

According to the obtained results, from finite element simulation, the following can be pointed out: Increasing the tightening torque, leads to a significant increase in the compressive stress in joints, as expected. The obtained results revealed that the amounts of resultant stresses were reduced by increasing the tightening torque due to compressive stresses which appeared around the hole by the compression of the plates by the bolt pretension. This can be, also, attributed to the method that the joint transmit the applied load. As the tightening torque is increased, a large part of the load is transmitted by friction (at the plate faces).

In addition, in the hybrid joints, the stress concentration around the hole is reduced significantly. As a result, the local stress at the edge of the hole is lower, since some portion of the total load is transmitted by adhesive layer.

Finally, the comparison of the obtained results, confirms that the hybrid joints have better static strength than simple joints for all levels of the tightening torque.

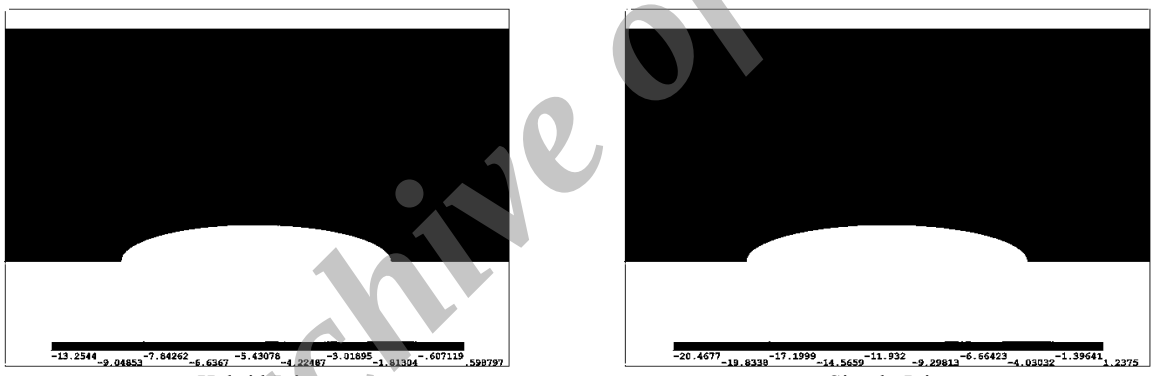

Hybrid Joint Simple Joint

(a) Clamped by T=1 Nm

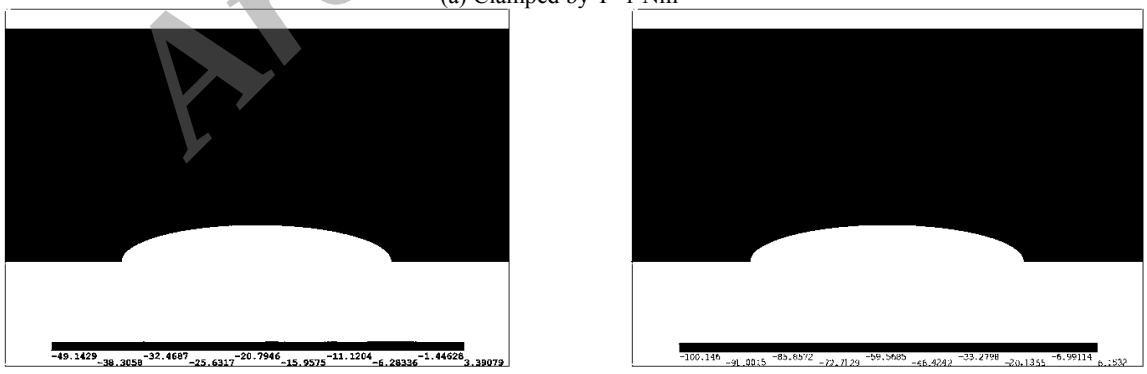

Hybrid Joint Simple Joint

(b) Clamped by T=5 Nm

Fig.12
Distribution of resultant compressive stress σ_z in MPa due to tightening torque of (a) 1 Nm, and (b) 5 Nm for simple and hybrid joints.

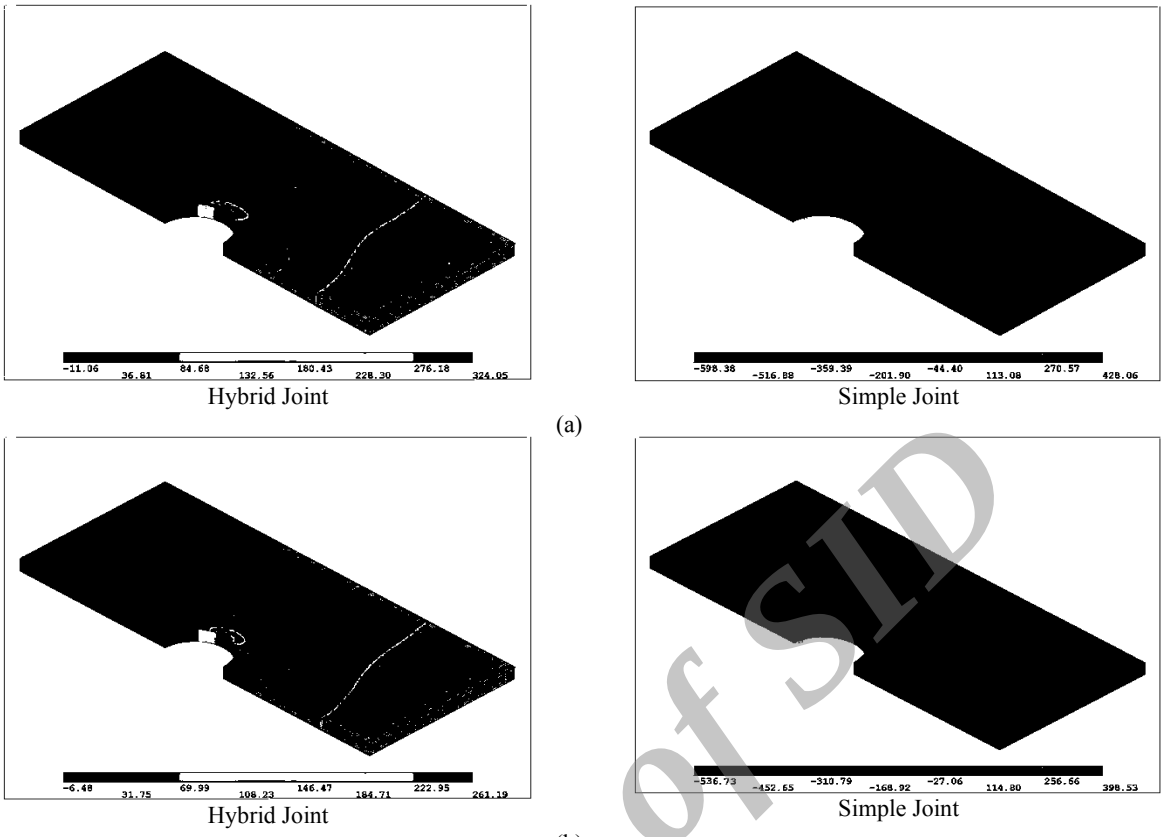

Fig.13
Distribution of longitudinal normal stress σ_x in MPa due to tightening torque (a) T=1 Nm, and (b) T=5 Nm and applied remote longitudinal tensile stress of 192 MPa.

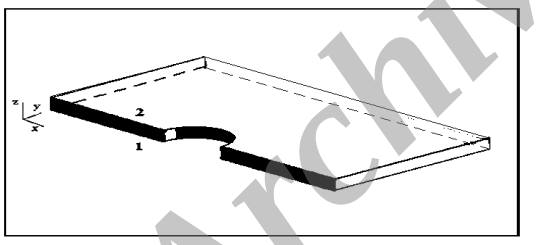

Fig.14
Typical nominating for selected paths on the main plate.

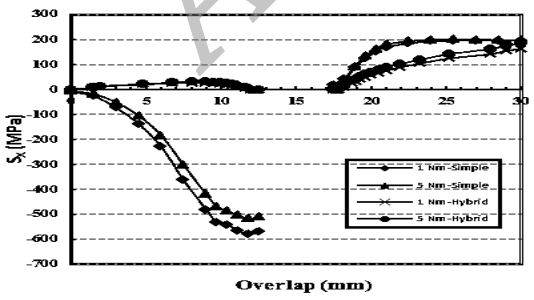

Path1

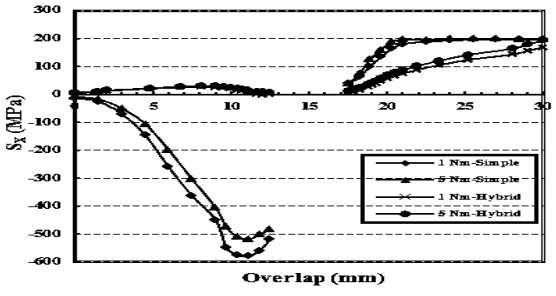

Path2

Fig.15
Distribution of longitudinal stress σ_x after clamping for different paths (a) Path 1, (b) Path 2; subjected to remote longitudinal tensile stress of 192 MPa.

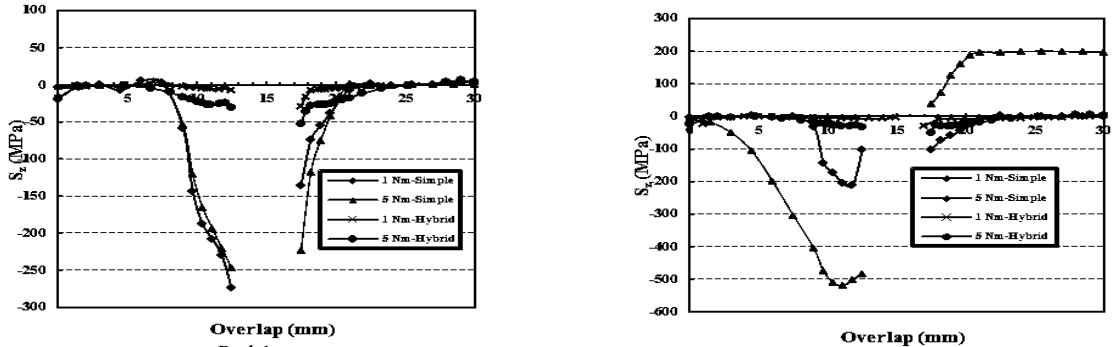

Path1 Path2

Fig.16

Distribution of Normal stress σ_z after clamping for different paths (a) Path 1, (b) Path 2; subjected to remote longitudinal tensile stress of 192 MPa.

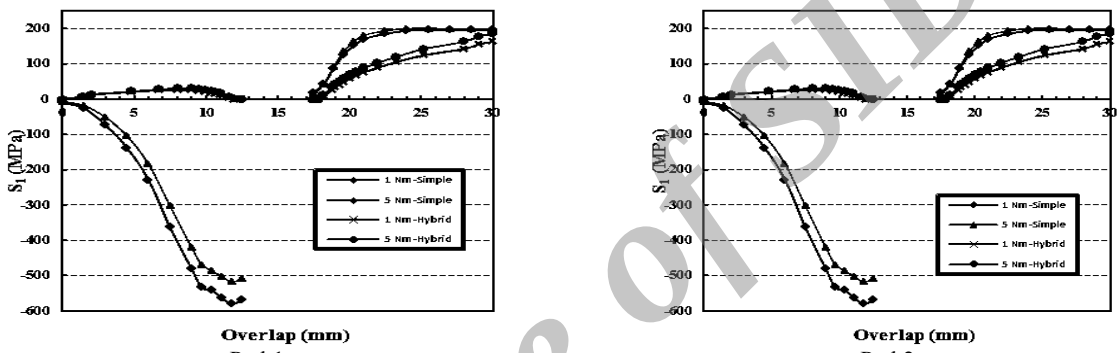

Path1 Path2

Fig.17

Distribution of first principal stress σ_1 after clamping for different paths (a) Path 1, (b) Path 2; subjected to remote longitudinal tensile stress of 192 MPa**.**

5 CONCLUSIONS

In the first part of present research, in order to evaluate the magnitude of the bolt preload or clamping force as a result of the applied tightening torque in double lap simple bolted and hybrid joints, an experimental approach has been used. To do so, a bolt transducer which positioned between the plate and nut was used. This bolt transducer consists of a hollow cylinder with two strain gages attached on its outer surface. The suitable strain gauge indicators were used to read the strains values of the attached strain gauges as a result of the induced axial strain from the torque tightening and therefore pretension or clamping force of bolts was calculated by means of Hooke's elasticity law. Lastly, the axial force in the hollow cylinder and then the clamping force have been determined.

The obtained results revealed that the clamping force due to a specific value of tightening torque in hybrid joints is lower than the obtained clamping force at the same value of tightening torque in simple bolted joints. In addition, it can be found that the torque coefficient increases from 0.202 to 0.238, for the simple bolted and hybrid joints, respectively.

In another part of this study, the effects of torque tightening on the stress distribution in double lap simple bolted and hybrid joints have been investigated numerically. To do so, three-dimensional finite element analyses with geometric and material nonlinearities have been carried out to obtain the stress distribution in joint plates due to clamping force and longitudinal applied loads and to afford a detailed clarification of the joint's performance. Two values of tightening torques were chosen to be applied to the bolt for tightening the joint. In a general trend, the amounts of resultant stresses were reduced by increasing the tightening torque due to compressive stresses which appeared around the hole by the compression of the plates by the bolt pretension. Furthermore, in the hybrid joints, the stress concentration around the hole is reduced significantly.

Because the stress distributions near the hole in the hybrid joints are relatively uniform in comparison with those in the simple bolted joints, the stress concentrations that occur near the edge of the holes in the hybrid joints are also reduced when using adhesive bonding in combination with mechanical fastening.

It must be mentioned that, despite all the work done in this study there are some points that can be evaluated in future works including the study of the effect of study the effect of adherend and adhesive geometry, elastic modulus of adhesive, adherend type and the effect of adhesion failures on stress distribution of hybrid joints.

REFERENCES

[1] Esmaeili F., Chakherlou T.N., Zehsaz M., 2014, Prediction of fatigue life in aircraft double lap bolted joints using several multiaxial fatigue criteria, *Materials and Design* **59**: 430-438.

[2] Esmaeili F., Chakherlou T.N., Zehsaz M., Hasanifard S., 2013, Investigating the effect of clamping force on the fatigue life of bolted plates using volumetric approach, *Journal of Mechanical Science and Technology* **27**(12):3657-3664.

[3] Iancu F., Ding X., Cloud G.L., Raju B.B., Hahn G.T., 2005, Three-dimensional investigation of thick single-lap bolted joints, *Experimental Mechanics* **45**(4): 351-358.

[4] Essam A., Bahkali A., 2011, Finite element modeling for thermal stresses developed in riveted and rivet-bonded joints, *International Journal of Engineering & Technology IJET-IJENS* **11**(6): 106-112.

[5] Fu M., Mallick P.K., 2001, Fatigue of hybrid (adhesive/bolted) joints in SRIM composites, *International Journal of Adhesion and Adhesives* **21**(2): 145-159.

[6] Gomez S., Onoro J., Pecharroman J., 2007, A simple mechanical model of a structural hybrid adhesive/riveted single lap joint, *International Journal of Adhesion and Adhesives* **27**(4): 263-267.

[7] Hart-Smith L.J., 1985, Bonded-bolted composite joints, *Journal of Aircraft* **22**(11): 993-1000.

[8] Allan R.C., Bird J., Clarke J.D., 1988, Use of adhesives in repair of cracks in ship structures, *Materials Science and Technology* **4**(10): 853-859.

[9] Camanho P.P., Tavares C.M.L., Oliveira R.d., Marques A.T., Ferreira A.J.M., 2005, Increasing the efficiency of composite single-shear lap joints using bonded inserts, *Composites Part B: Engineering* **36**(5): 372-383.

[10] Chan W.S., Vedhagiri S., 2001, Analysis of composite bonded/bolted joints used in repairing, *Journal of Composite Materials* **35**(12): 1045-1061.

[11] Kelly G., 2005, Load transfer in hybrid (bonded/bolted) composite single-lap joints, *Composite Structures* **69**(1): 35-43.

[12] Barut A., Madenci E., 2009, Analysis of bolted-bonded composite single-lap joints under combined in-plane and transverse loading, *Composite Structures* **88**(4): 579-594.

[13] Paroissien E., Sartor M., Huet J., Lachaud F., 2007, Analytical two-dimensional model of a hybrid (bolted/bonded) single-lap joint, *Journal of Aircraft* **44**(2): 573-582.

[14] Sugaya T., Obuchi T., Chiaki S., 2011, Influences of loading rates on stress-strain relations of cured bulks of brittle and ductile adhesives, *Journal of Solid Mechanics and Materials Engineering* **5**(12): 921-928.

[15] Kweon J., Jung J., Kim T., Chai J., Kim D., 2006, Failure of carbon composite-to aluminum joints with combined mechanical fastening and adhesive bonding, *Composite Structures* **75**(1-4): 192-198.

[16] Iyer K., Rubin C.A., Hahn G.T., 2001, Influence of interference and clamping on fretting fatigue in single rivet-row lap joints, *Journal of Tribology-transactions of the ASME* **123**(4): 686-698.

[17] Aragon A., Alegre J.M., Gutierrez-Solana F., 2006, Effect of clamping force on the fatigue behaviour of punched plates subjected to axial loading, *Engineering Failure Analysis* **13**(2): 271-281.

[18] Sekercioglu T., Kovan V., 2008, Torque strength of bolted connections with locked anaerobic adhesive, *Proceedings of the Institution of Mechanical Engineers, Journal of Materials: Design and Applications* **222** (1): 83-90.

[19] Chakherlou T.N., Abazadeh B., Vogwell J., 2009, The effect of bolt clamping force on the fracture strength and the stress intensity factor of a plate containing a fastener hole with edge cracks, *Engineering Failure Analysis* **16**(1): 242-253.

[20] Oskouei R.H., Chakherlou T.N., 2009, Reduction in clamping force due to applied longitudinal load to aerospace Structural bolted plates, *Aerospace Science and Technology* **13**(6): 325-330.

[21] Budynas R.G., Nisbett J.K., 2011, *Shigley's Mechanical Engineering Design*, McGraw-Hill.

[22] Chakherlou T.N., Alvandi-Tabrizi Y., Kiani A., 2011, On the fatigue behavior of cold expanded fastener holes subjected to bolt tightening, *International Journal of Fatigue* **33**(6): 800-810.

[23] Collings T.A., 1977, The strength of bolted joints in multi-directional CFRP laminates, *Composites* **8**(1): 43-54.

[24] Stockdale J.H., Matthews F.L., 1976, The effect of clamping pressure on bolt bearing loads in glass fiber-reinforced plastics, *Composites* **7**(1): 34-39.

[25] Deng X., Hutchinson J.W., 1998, The Clamping Stress in a Cold Driven Rivet, *International Journal of Mechanical Sciences* **40**(7): 683-694.

[26] Nah H.S., Lee H.J., Kim K.S., Kim J.H., Kim W.B., 2009, Method for estimating the clamping force of high strength bolts subjected to temperature variation, *International Journal of Steel Structures* **9**(2): 123-130.

[27] Technical Data Sheet, 2003, Product 3421, Loctite Corp, Dublin.

[28] Oskouei R.H., 2005, An investigation into bolt clamping effects on distributions of stresses and strains near fastener hole and its effect on fatigue life, MSc thesis, University of Tabriz, Tabriz, Iran.
[29] Swanson Analysis Systems Inc,2004, ANSYS, Release 9.
[30] De Angelis F., 2012, A comparative analysis of linear and nonlinear kinematic hardening rules in computational elastoplasticity, *Technische Mechanik* **32** (2-5):164-173.
[31] De Angelis F., 2000, An internal variable variational formulation of viscoplasticity, *Computer Methods in Applied Mechanics and Engineering* **190**(1-2) : 35-54.
[32] De Angelis F., 2007, A variationally consistent formulation of nonlocal plasticity, *Journal for Multiscale Computational Engineering* **5** (2):105-116.